THE JOURNAL OF PHYSICAL CHEMISTRY LETTERS
A JOURNAL OF THE AMERICAN CHEMICAL SOCIETY

pubs.acs.org/JPCL Letter

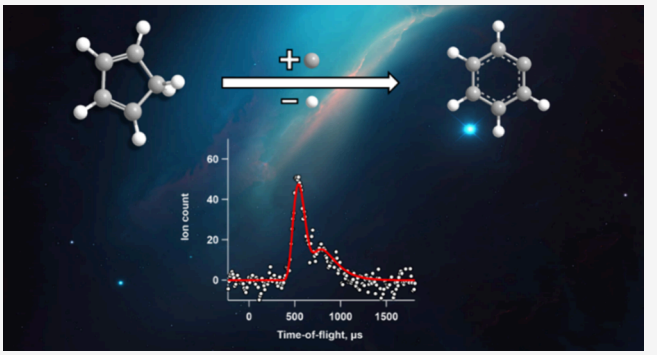
Barrierless Gas-Phase Formation of the Phenyl Radical (C_6H_5, X^2A_1) via Atomic Carbon Induced Ring Expansion—A Versatile Framework to Hückel Aromatic Aryl Radicals in Molecular Clouds

Daniel González, Ashleigh G. Hartwig, Surajit Metya, Iakov A. Medvedkov, Shane J. Goettl, Alexander M. Mebel,* and Ralf I. Kaiser*

Cite This: *J. Phys. Chem. Lett.* 2026, 17, 12367−12375 Read Online

ACCESS | Metrics & More | Article Recommendations | Supporting Information

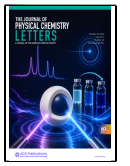
ABSTRACT: The low-temperature formation of aromatic molecules in the interstellar medium remains a major challenge in astrochemistry. Here, crossed molecular beam experiments combined with high-level electronic structure and Rice−Ramsperger−Kassel−Marcus (RRKM) calculations reveal the barrierless formation of the simplest aryl radical, the 6π Hückel aromatic phenyl radical ($C_6H_5^{\bullet}$), through the reaction of ground-state atomic carbon with 1,3-cyclopentadiene (c-C_5H_6). The reaction proceeds via carbon addition, ring expansion, hydrogen atom elimination, and aromatization, with all transition states lying below the energy of the separated reactants. The measured reaction exoergicity agrees with theory, rendering the reaction operative even in the coldest interstellar environments. More broadly, carbon-atom-induced ring-expansion can transform cyclopentadiene motifs embedded within larger polycyclic aromatic hydrocarbons into aryl radical centers, providing a previously unrecognized route to aromatic molecular growth. These findings establish carbon-atom-mediated skeletal editing as a viable low-temperature mechanism for building increasingly complex aromatic carbonaceous molecules in space.



The formation and persistence of aromatic hydrocarbons in low-temperature extraterrestrial environments remains an unresolved challenge in astrochemistry.[1,2] In particular, polycyclic aromatic hydrocarbons (PAHs), organic compounds characterized by multiple fused aromatic rings with delocalized π-electrons as complex as substituted coronene,[3] have been widely detected throughout the interstellar medium as well as in carbonaceous meteorites like Murchison[4] and asteroids such as Bennu.[5,6] Yet, their observed abundances contrasts modeling predictions with predicted fractions up to 3 orders of magnitude lower than observations.[1,7] Further, expected life times of PAHs in deep space of some 10^8 years[7−11] are in stark contrast to modeled production rates of 10^9 years,[11] suggesting that interstellar PAHs are destroyed faster than they can be replenished;[7,11−15] in other words, PAHs should not exist in molecular clouds at all. This apparent imbalance implies that efficient growth pathways capable of continuously regenerating aromatic complexity under extreme temperatures as low as 10 K are still missing.[2,15] Here, the phenyl radical ($C_6H_5^{\bullet}$, X^2A_1) has emerged as a fundamental precursor in aromatic molecular mass growth processes and potential key intermediate in resolving the aforementioned paradox.[16] As the smallest aryl radical, the 6π Hückel aromatic phenyl occupies a unique position at the interface between one-ringed aromatics hydrocarbons and larger ring systems such as PAHs.

Phenyl-driven growth pathways have been shown to produce PAHs through reactions with unsaturated hydrocarbons.[17,18] For instance, the reaction between phenyl radicals and vinylacetylene (C_4H_4, X^1A') offers an efficient and barrierless gas-phase route to naphthalene ($C_{10}H_8$, X^1A_g) via the hydrogen abstraction−vinylacetylene addition (HAVA) mechanism.[17,19] This step represents a critical transition from monocyclic to fused aromatic structures and establishes a foundation for subsequent ring-expansion and annulation processes that generates increasingly complex PAH architectures.[17] In addition to promoting the growth of planar PAH frameworks,[20,21] phenyl radicals ($C_6H_5^{\bullet}$) also participate in reaction pathways that generate five-membered ring-containing PAHs, including acenaphthylene ($C_{12}H_8$, X^1A'),[22] fluorene ($C_{13}H_{10}$,

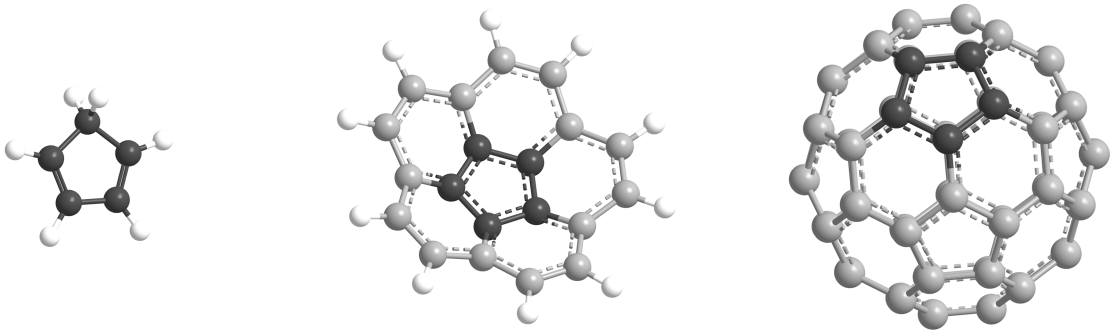
Received: September 10, 2026
Revised: September 30, 2026
Accepted: October 6, 2026
Published: October 14, 2026



ACS Publications
© 2026 The Authors. Published by American Chemical Society

https://doi.org/10.1021/acs.jpclett.6c03038
J. Phys. Chem. Lett. 2026, 17, 12367−12375

Scheme 1. Molecular Structures of Cyclopentadiene (C_5H_6) along with Nonplanar Corannulene ($C_{20}H_{10}$) and Buckminsterfullerene (C_{60}) PAHs Carrying Five-Membered Ring(s)[a]



Cyclopentadiene (C_5H_6) Corannulene ($C_{20}H_{10}$) Buckminsterfullerene (C_{60})

[a]Carbon atoms of the cyclopentadiene moiety are color coded in black, while the remaining carbon and hydrogen atoms are shown in gray and white, respectively.

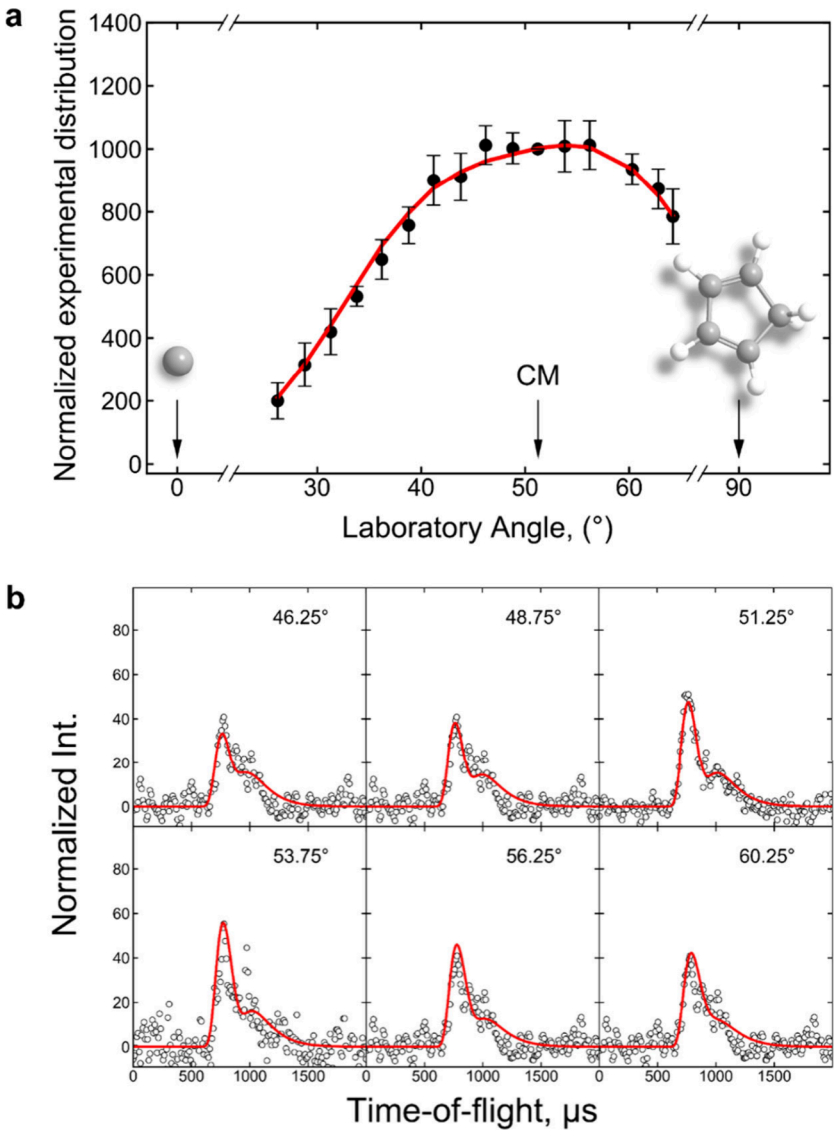


Figure 1. (a) Laboratory angular distribution and (b) time-of-flight (TOF) spectra recorded at mass to charge (m/z) of 76 for the reaction of ground state carbon atoms (C, ^3P) with 1,3-cyclopentadiene (c-C_5H_6, X^1A_1). CM represents the center-of-mass angle, and 0° and 90° define the directions of the carbon atom and 1,3-cyclopentadiene beams, respectively. The black circles depict the experimental data and red lines the fits. Atoms are colored as follows: carbon (gray) and hydrogen (white).

https://doi.org/10.1021/acs.jpclett.6c03038
J. Phys. Chem. Lett. 2026, 17, 12367−12375

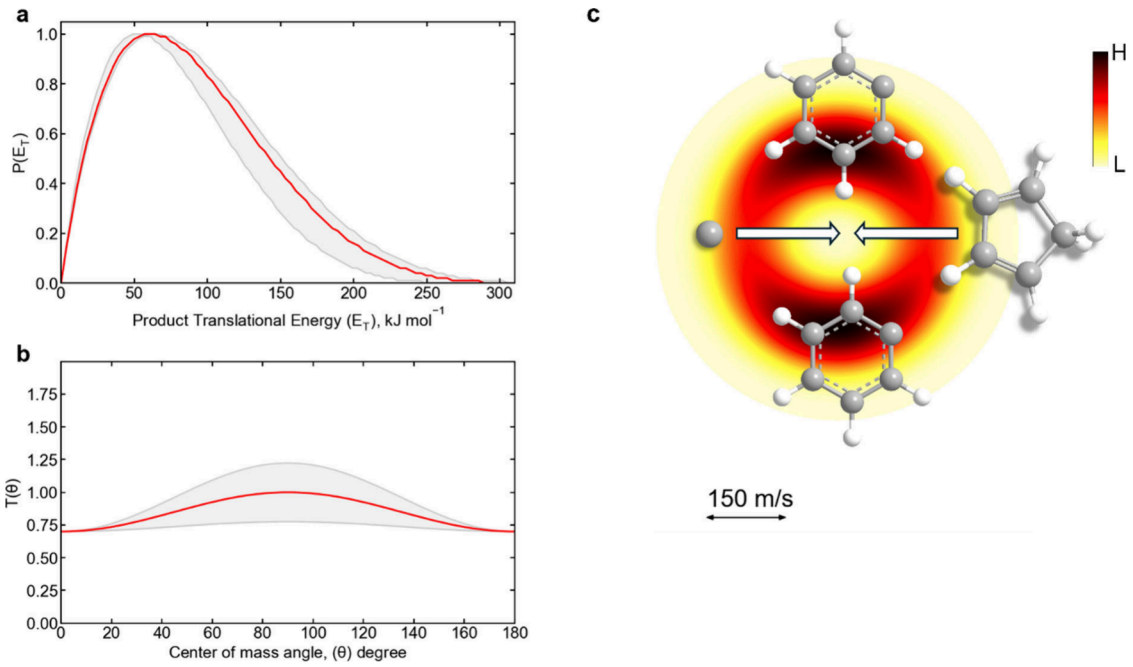


Figure 2. (a) CM translational energy ($P(E_T)$) and (b) angular flux distributions ($T(\theta)$), as well as (c) the associated flux contour map for the reaction of ground state atomic carbon (C, ^{3}P) with 1,3-cyclopentadiene (c-C_5H_6, X^1A_1). The red solid lines in (a) and (b) define the best-fit functions while shaded areas provide the error limits. For the $T(\theta)$, the direction of the C beam is defined as 0° and of the c-C_5H_6 as 180°. The flux contour map represents the intensity of the reactively scattered products as a function of product velocity (u) and scattering angle (θ), and the color bar indicates flux gradient from high (H) to low (L) intensity. Atoms are colored as follows: carbon (gray) and hydrogen (white).

X^1A_1),[23] and fluoranthene ($C_{16}H_{10}$, X^1A').[24] The incorporation of the cyclopentadiene moieties represents a key step toward the formation of curved aromatic structures, providing access to nonplanar bowl-shaped PAHs such as corannulene and, ultimately, fullerenes (Scheme 1).[23,24] Thus, the phenyl radicals ($C_6H_5^\bullet$) represent a fundamental entry point into both planar and three-dimensional carbonaceous materials formation in astrophysical environments. Nevertheless, the processes leading to the synthesis of the phenyl radicals may hardly be photochemically initiated in the low-temperature regions such as dense molecular clouds, where ultraviolet (UV) photons are predominantly shielded and are scarce. Previous studies have shown that viable routes including the reaction of dicarbon (C_2, $X^1\Sigma_g^+/a^3\Pi_u$) with 1,3-butadiene (C_4H_6, X^1A_g) under single-collision conditions,[25] as well as the propargyl radical ($C_3H_3^\bullet$, X^2B_1) self-reaction using isomer-selective synchrotron mass spectrometry,[26] might be responsible for the phenyl radicals ($C_6H_5^\bullet$) formation in these low-temperature environments. Consequently, identifying elementary reactions governing the phenyl radical production and trigger their subsequent chemistry is essential for understanding the chemical evolution of our universe. Inspired by the works demonstrating that ground-state atomic carbon (C, ^{3}P) reacts barrierlessly with unsaturated hydrocarbons[27−29] we untangle the chemical dynamics the bimolecular gas-phase reaction of ground-state carbon atoms (C, ^{3}P) with 1,3-cyclopentadiene (c-C_5H_6; X^1A_1) under single-collision conditions using the crossed molecular beam technique coupled to universal mass spectrometric product detection, allowing the observation of the phenyl radical under single collision conditions. Along with previous kinetic measurements of the carbon − cyclopentadiene reaction, holding a rate constant of 1.9×10^{-9} cm^3 s^{-1} at 300 K,[30] and the exoergic and barrierless nature of the synthesis of the phenyl radical, the title reaction provides a potential route to interstellar phenyl radicals even in the coldest and darkest regions of the deep space. Overall, upon reaction with cyclopentadiene motifs in PAHs, atomic carbon may induce ring expansion of into aromatic aryl radicals thus providing a versatile, carbon-atom-mediated skeletal editing of aromatic precursors to progressively larger aryl radicals, thereby establishing a new paradigm for aromatic molecular growth in low-temperature astrochemical environments.

The reactive scattering experiments for the reaction between ground-state atomic carbon (C, ^{3}P) and 1,3-cyclopentadiene (c-C_5H_6; X^1A_1) were performed in the gas-phase under single-collision conditions (Methods). Signal was detected at mass-to-charge (m/z) ratios of 77 ($C_6H_5^+$) (1) and 76 ($C_6H_4^+$) (2). The TOF profiles at both masses were indistinguishable (Figure S1), revealing that signal arises from $C_6H_5^\bullet$ radicals (77 amu) plus a hydrogen atom (1 amu) (reaction 1); signal at m/z = 76 is attributed to dissociative ionization of the parent species inside the electron impact ionizer located within the detector region. Although the reaction 2 cannot be excluded, no distinct contribution from this channel could be resolved under the present experimental conditions. Due to the slightly higher signal-to-noise ratio observed at m/z = 76, this m/z was selected for detailed analysis and TOF spectra were collected over a laboratory angular range from 26.25° and 56.25° in 2.5° increments, and at 60.25°, 62.75° and 64.25°. These spectra were subsequently integrated and normalized with respect to the TOF recorded at the center-of-mass (CM) angle, to derive the laboratory angular distribution (LAD) (Figure 1). The resulting LAD exhibits near forward−backward symmetry with a broad maximum around the CM angle. Such a distribution is characteristic of indirect scattering dynamics, involving the formation of relatively long-lived C_6H_6 intermediate complex(es) that ultimately dissociate via hydrogen atom elimination yielding $C_6H_5^\bullet$ products.[31,32] Together, these results demon-

https://doi.org/10.1021/acs.jpclett.6c03038
J. Phys. Chem. Lett. 2026, 17, 12367−12375

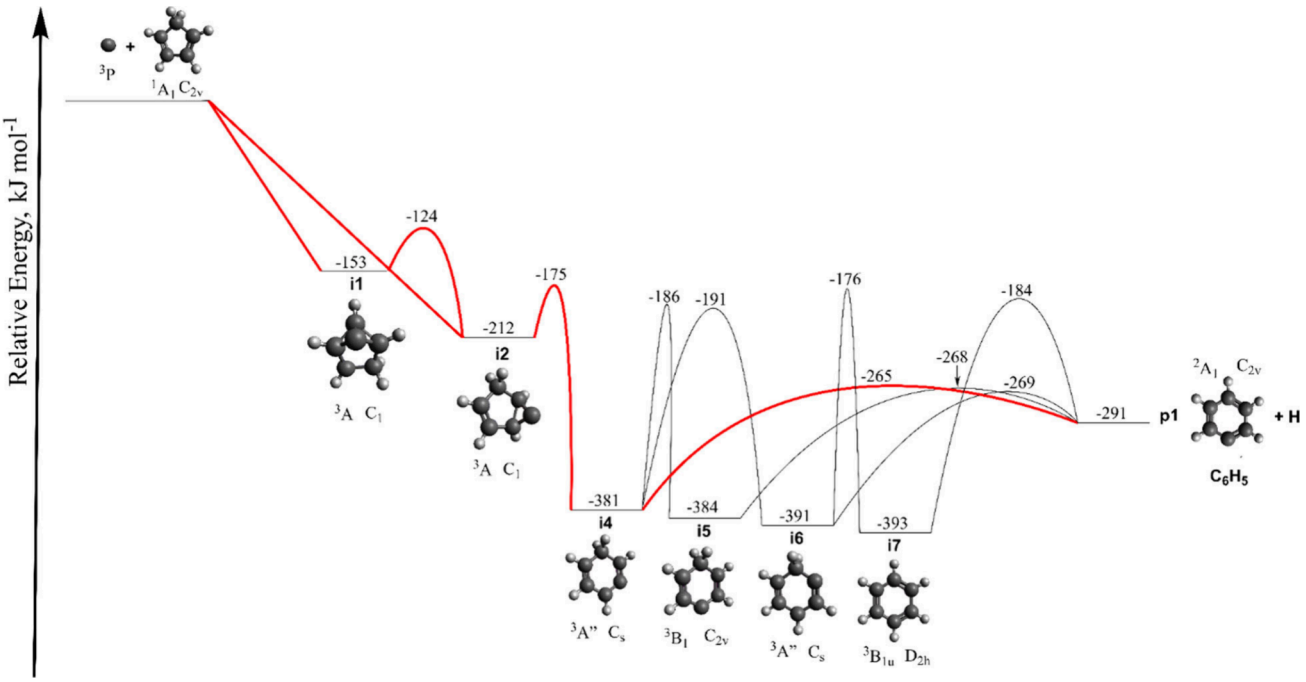


Figure 3. Schematic potential energy surface for the reaction of carbon atoms (C, ^{3}P) and 1,3-cyclopentadiene (c-C_5H_6, X^1A_1) obtained at a level of CCSD(T)-F12/cc-pVQZ-F12//ωB97X-D/6-311G(d,p) + ZPE(ωB97X-D/6-311G(d,p)), leading to the phenyl radical, **p1** (C_6H_5, X^2A_1). Red color line represents the most probable pathways to **p1**.

strate that the title reaction proceeds through an atomic carbon versus hydrogen exchange mechanism, enabling the formation of C_6H_5• isomer(s).

$$\mathrm{C(12\ amu) + c\text{-}C_5H_6(66\ amu)} \rightarrow \mathrm{C_6H_5(77\ amu) + H(1\ amu)} \quad (1)$$

$$\mathrm{C(12\ amu) + c\text{-}C_5H_6(66\ amu)} \rightarrow \mathrm{C_6H_4(76\ amu) + H_2(2\ amu)} \quad (2)$$

The identification of $C_6H_5^•$ isomer(s) enables an investigation of their structures and formation mechanism. To this end, the laboratory-frame data (TOF spectra and LADs) were transformed into the center of mass (CM) reference frame to derive the translational energy, $P(E_T)$, and angular flux, $T(\theta)$, distributions (Figure 2).[27,33] The laboratory data are reproduced by a single reaction channel (reaction 1) involving an atomic hydrogen loss channel. The $P(E_T)$ distribution exhibits a maximum at 59 ± 6 kJ mol^{-1}, indicative of a tight exit transition state in the unimolecular decomposition of the C_6H_6 intermediate(s). The high-energy cutoff, E_{max} = 281 ± 30 kJ mol^{-1}, corresponds to the sum of the reaction exoergicity and the collision energy (22.0 ± 0.7 kJ mol^{-1}) for those products formed without internal excitation. This yields a reaction exoergicity of 259 ± 30 kJ mol^{-1}. In addition, fractions of 32 ± 7% of the total available energy are partitioned into product translation supporting an indirect reaction mechanism.[32] The $T(\theta)$ distribution exhibits a forward−backward symmetry with a maximum at 90° (Figure 2b), indicative of sideways scattering. These patterns reveal indirect dynamics involving long-lived C_6H_6 intermediates, whose lifetimes are comparable to or exceed their rotational periods.[27] This feature further suggests geometrical constraints that favor hydrogen atom emission nearly parallel to the total angular momentum vector, *i.e.*, perpendicular to the rotational plane of the decomposing complex. This behavior is also reflected in the corresponding flux contour map (Figure 2c).

The formation of $C_6H_5^•$ isomer(s) under single-collision conditions prompted a computational analysis of the carbon, cyclopentadiene system to determine the structure of the reaction products and to reveal the mechanisms responsible for their formation. Accordingly, electronic structure calculations, accurate within 5 kJ mol^{-1}, were performed together with Rice−Ramsperger−Kassel−Marcus (RRKM) calculations to evaluate unimolecular rate constants and product branching fractions (Tables S2 and S3). The complete potential energy surface (PES) is available in the Supporting Information (Figure S2); intermediates **i3** and **i8** have been omitted from Figure 3 since they resemble "dead end" intermediates. The PES exposes the production of the phenyl radical (**p1**, C_{2v}, X^2A_1) formed with a computed reaction energy of −291 ± 5 kJ mol^{-1}. The experimentally determined reaction energy of −259 ± 30 kJ mol^{-1} is in good agreement, within the error limits, with the calculated exoergicity for the phenyl radical. Furthermore, these values compare favorably with the reaction energy of −294 ± 1 kJ mol^{-1} based on the experimental formation enthalpies taken from Active Thermochemical Tables (ATcT).[34] Overall, the combined experimental and theoretical evidence points to the formation of phenyl radical in the carbon − cyclopentadiene system. Yet, what is the reaction mechanism leading to **p1**? According to the theoretical investigation, the synthesis of the phenyl radicals is initiated on the triplet surface by the barrierless addition of the ground state atomic carbon through simultaneous addition across single and double carbon−carbon bonds or through addition to only one of the double bonds. This leads to the formation of the triplet tricyclo[3.1.0.0^{2,6}] hexane-1,3-diyl intermediate **i1** (C_1, X^3A) and the bicyclo[3.1.0]hex-2-ene-6-ylidene **i2** (C_1, X^3A), stabilized by 153 and 212 kJ mol^{-1} relative to the separated reactants, respectively. Both

https://doi.org/10.1021/acs.jpclett.6c03038
J. Phys. Chem. Lett. 2026, 17, 12367−12375

intermediates are interconnected by a barrier of only 29 kJ mol^{-1}. Note that **i2** structural analogs have also been computed in previous carbon systems involving unsaturated (acetylene (C_2H_2),[35] ethylene (C_2H_4),[35] propargyl radical ($^{\bullet}C_3H_3$),[36] methylacetylene (C_3H_4),[29,35] propylene (C_3H_6),[35] acetylene (C_4H_2),[37] vinylacetylene (C_4H_4),[38] 1,3-butadiene ($H_2CCHCHCH_2$),[39] dimethylacetylene (H_3CCCCH_3),[40] and benzene (C_6H_6),[41] styrene ($C_6H_5CHCH_2$),[42] indene (C_9H_8[43]) hydrocarbons under single-collision conditions. From **i2**, a ring opening of the three-membered ring over a moderate barrier of 37 kJ mol^{-1} generates the six-membered cyclic intermediate **i4** (C_s, X^3A''), thereby establishing the benzene carbon framework. Once formed, **i4** can undergo hydrogen atom elimination to **p1** overcoming a tight exit transition state lying 23 kJ mol^{-1} above **p1**. Alternatively, **i4** may isomerize through hydrogen migrations to either **i5** (C_{2v}, X^3B_1) or **i6** (C_s, X^3A''), involving substantial barriers of 195 kJ mol^{-1} and 190 kJ mol^{-1}, respectively. An additional hydrogen shift from **i6** yields to triplet benzene, **i7** (D_{2h}, X^3B_{1u}) with an associated significant barrier of 215 kJ mol^{-1}. **i5**, **i6**, and **i7** serve as precursors to the phenyl radical product, **p1** plus atomic hydrogen, through tight exit transition states located 23, 22, and 107 kJ mol^{-1} above **p1**. These computational results are in agreement with the experimental findings, which likewise suggest the presence of tight exit transition states governing the hydrogen atom loss.

It should be noted that we did not consider triplet-to-singlet intersystem crossing (ISX) in the present system and fully focused only on the triplet PES. The neglection of ISX and consequently the singlet surface is justified because hydrocarbons typically have very low spin−orbit coupling and hence, ISX could be feasible only for long-lived intermediates. According to RRKM-calculated rate constants (Table S2), lifetimes of **i2** and **i4** are in the range of 1−10 ps (10^{-12} s). Rate constants for ISX evaluated earlier for the prototype cyclopropylidene and similar carbene and triplet structures of C_3H_2 are on the order 10^9 s^{-1}, i.e., 2−3 orders of magnitude lower compared to those for isomerization or decomposition of **i2** and **i4**.[44] More recently, we found that ISX is generally not competitive as compared with isomerization and dissociation on the triplet surface in a larger polycyclic aromatic $C_{15}H_{10}$ molecule with rate constants being on the order of 10^7−10^8 s^{-1}.[45]

The discussion now shifts to elucidating the most probable reaction pathway for the formation of **p1**. We can ignore alternative C_6H_5 isomers other than phenyl here because they lie much higher in energy. For example, a removal of H from the CH_2 group in either **i1** or **i2** leads to a radical of benzvalene (benzvalenyl) which is ∼270 kJ mol^{-1} higher in energy than phenyl. H losses from CH groups in **i4**−**i6** give radicals ∼240−260 kJ mol^{-1} less stable than phenyl. Considering short lifetimes of **i1** and **i2** with respect to their isomerization and of **i4**−**i6** with respect to their decomposition to **p1** + H, highly energetically demanding formation of the other C_6H_5 isomers is not competitive. Also, open-ring C_6H_5 isomers were earlier reported to reside 255−258 kJ mol^{-1} above phenyl[46] and hence, pathways involving ring-opening would be unlikely. Therefore, **p1** represents the practically exclusive C_6H_5 product. Based on the barriers, the most feasible route to form phenyl radicals follows through the unimolecular decomposition of **i4**. Further, the synthesis of **p1** from **i5**, **i6**, and **i7** requires surmounting considerable barriers of about 200 kJ mol^{-1}, hindering the pathways involving these intermediates to contribute significantly to $C_6H_5^{\bullet}$ production. To shed light on this question, a RRKM statistical analysis was also performed to calculate the contribution of the intermediates **i4**−**i7** to the phenyl radicals (**p1**) formation at two different collision energies corresponding to the experimental conditions (E_c = 22.0 kJ mol^{-1}) and to the low temperatures of the cold molecular clouds (E_c = 0 kJ mol^{-1}) (Table S2). The final results corroborated the predicted behavior, regardless the collision energy considered, with **i4** being almost the exclusive contributor to **p1** production. In contrast, insignificant fractions of less than 0.5% were calculated for **i5**−**i7** intermediates to form **p1**, in the best scenario. In addition, a closer inspection of the calculated geometries of the exit transition states also provides additional insight into the underlying reaction mechanism. The exit transition states connecting **i4**, **i5** and **i6** to **p1** (**i4** → **p1** + H, **i5** → **p1** + H and **i6** → **p1** + H) reveal that the departing hydrogen atom is emitted nearly perpendicular to the plane of the rotating complex, with angles ranging from 71.0° to 72.4° (Figure 4). This finding is consistent with the sideways

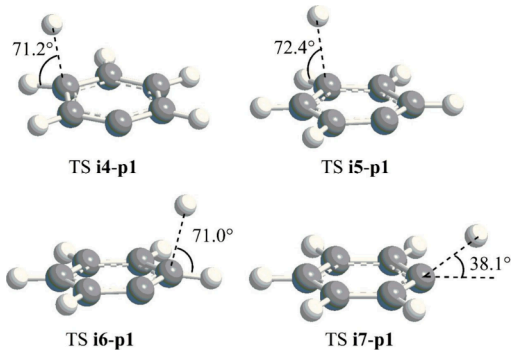


Figure 4. Computed geometries of the exit transition states leading to the phenyl radical, **p1** (C_6H_5, X^2A_1). Angles of the departing hydrogen atoms are given in degrees with respect to the rotation plane of the decomposing complex.

scattering observed in the $T(\theta)$ distributions obtained from the experimental results. On the other hand, the corresponding exit transition state from **i7** (**i7** → **p1** + H) does not display this perpendicular emission geometry, with an angle of 38.1° for the hydrogen atom emission, lending further support to the negligible role of this pathway to the formation of **p1**, as discussed above. In summary, the barrierless formation of the phenyl radical (**p1**) commences on the triplet surface from the initial collision complexes **i2** or **i1**, which undergoes a facile isomerization to **i2**. Subsequent ring opening of **i2** yields **i4**, thus assembling the carbon backbone of benzene. Finally, loss of an atomic hydrogen followed by aromatization of the methylene group then produces the phenyl radical via a tight exit transition state (Figure 3).

To sum up, the present study reveals a barrierless mechanism for the conversion of cyclopentadiene into the simplest aryl radical, phenyl radical, via atomic carbon addition−hydrogen loss elimination (Figure 5a). Consistent with this mechanism, the previously measured rate coefficient is closed to the gas-kinetics limit (1.9×10^{-9} cm^3 s^{-1}),[30] comparable to a few 10^{-10} cm^3 s^{-1} reported for reactions of atomic carbon with other unsaturated hydrocarbons such as acetylene (C_2H_2),[47] ethylene (C_2H_4),[47,48] propylene (C_3H_6),[47,48] or 1/2-butene (C_4H_8).[48] Furthermore, this

https://doi.org/10.1021/acs.jpclett.6c03038
J. Phys. Chem. Lett. 2026, 17, 12367−12375

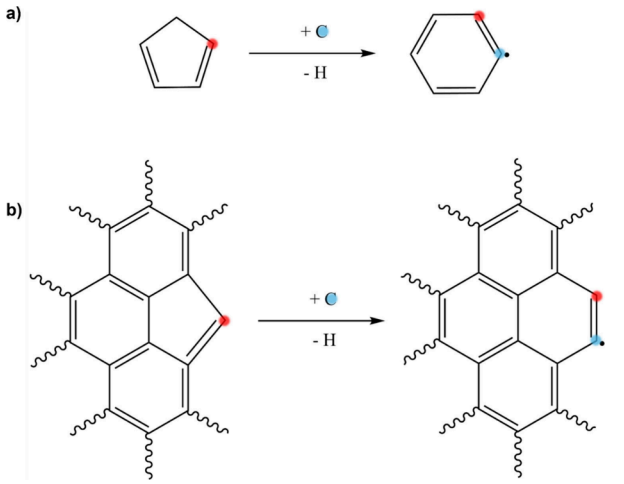


Figure 5. Schematic representation of the carbon addition−ring expansion of a cyclopentadiene moiety leading to aryl radicals. (a) Conversion of cyclopentadiene into the phenyl radical, and (b) analogous ring expansion of a cyclopentadiene moiety embedded within a larger PAH, leading to the formation of an aryl radical. The carbon centers of each reactant are represented by red and blue circles.

observation of an atomic carbon induced ring expansion is expected not to be restricted to one isolated cyclopentadiene molecule, but instead to represent a versatile transformation of cyclopentadiene moieties into aryl radicals (Figure 5b). A similar mechanistic pathway has also been reported for the reaction of atomic carbon with indene,[43] suggesting that this process may extend to cyclopentadiene units embedded within larger PAHs. Nevertheless, the general applicability of this mechanism to other PAH systems remains to be established. This finding is particularly significant since it allows the formation of large aryl radicals in low-temperature extraterrestrial environments, such as the cold molecular clouds, and initiate a reaction sequence contributing to the mass molecular growth processes of PAHs toward these extreme sources from cyclopentadiene moieties via aryl radicals followed by ring annulation through hydrogen abstraction−vinylacetylene addition (HAVA).[2,15,17,20,49,50] In addition, replacing the hydrogen atoms of cyclopentadiene (or larger five-membered ring-containing PAHs) by organic substituents, such as ethynyl (−CCH) or cyano (−CN) groups, is expected to produce the corresponding aryl-substituted species in low-temperature environments. These discoveries expand the current picture of interstellar aromatic chemistry by demonstrating that barrierless carbon additions followed by ring expansion can simultaneously drive molecular growth and structural reorganization. Such chemistry offers a previously overlooked mechanism for the transformation of simple hydrocarbons into increasingly complex aromatic architectures, providing new insight into the origin, evolution, and persistence of the aromatic molecular inventory throughout our carbon-rich Universe.

MATERIALS AND METHODS

The bimolecular gas-phase reaction between ground-state atomic carbon (C, ^{3}P) and 1,3-cyclopentadiene (c-C_5H_6; X^1A_1) was investigated under single-collision conditions using a crossed molecular beam apparatus combined with time-of-flight (TOF) mass spectrometric detection.[51] The supersonic beam of carbon atoms was generated *in situ* via laser ablation of a rotating graphite rod, employing the fourth harmonic (266 nm) output of a Nd:YAG laser (Quanta-Ray Pro 270, Spectra-Physics) operating at 30 Hz with a pulse energy around 8 mJ per pulse. The ablated carbon species were seeded in helium (He, 99.9999%, Airgas) carrier gas at a backing pressure of 4 atm, pulsed through a piezoelectric pulsed valve operating at 60 Hz. After passing through a 1 mm diameter skimmer, the beam was velocity-selected with a chopper wheel running at 120 Hz, producing a carbon beam with a peak velocity (v_p) of 2028 ± 26 m s^{-1} and a speed ratio (S) of 4.3 ± 0.2. The 1,3-cyclopentadiene (c-C_5H_6) reactant seeded at a fraction of 5% in krypton (99.9999%, Praxair) was expanded through a second piezoelectric pulsed valve at a backing pressure of 520 Torr to form a supersonic beam with a peak velocity of v_p = 464 ± 9 m s^{-1} and S = 17.6 ± 0.6. 1,3-cyclopentadiene was synthesized by cracking the dimer, dicyclopentadiene ($C_{10}H_{12}$), up to 180−190 °C and further purified by multiple freeze−pump−thaw cycles, prior to diluting it in krypton with a total pressure up to 0.68 atm.[52] The two beams intersected at a 90° angle within the interaction region, resulting in a collision energy (E_c) of 22.0 ± 0.7 kJ mol^{-1} and a center-of-mass angle of (θ_{CM}) of 52.2 ± 0.8°. Experimental parameters were carefully tuned to minimize the presence of dicarbon to levels <5% relative to atomic carbon in the primary beam.

Neutral reaction products entering the triply differentially pumped ultrahigh vacuum detector (6.6 × 10^{-12} Torr) were ionized by electron impact at 80 eV. The resulting ions were then mass-filtered using a quadrupole mass spectrometer (Extrel, QC 150, QPS, 2.1 MHz) operating in time-of-flight (TOF) mode. A detailed description of the detector setup is available elsewhere.[53] Briefly, the selected ions were accelerated toward a −22.5 kV target, initiating an electron cascade that ultimately produced a photon signal via an organic scintillator. This signal was detected using a Burle photomultiplier tube (−1.35 kV), processed with a discriminator set to 1.6 mV, and recorded by a multichannel scaler. The detector assembly can rotate within the plane defined by the intersecting beams, allowing measurements to be collected over a range of laboratory angles. Laboratory angular distribution (LADs) for selected mass-to-charge (m/z) ratios were obtained by integrating the TOF spectra and normalizing the signals to that measured at the center-of-mass (CM) angle.

Both the LADs and TOF spectra were subsequently converted into the CM reference frame using a forward-convolution approach to extract information on the reaction dynamics.[27,54,55] In this procedure, the CM translational energy distribution, $P(E_T)$, and the angular flux distribution, $T(\theta)$, were iteratively adjusted until the best agreement with the experimental data was achieved. The reactive differential cross section, expressed as $I(u,\theta) \sim P(u) \times T(\theta)$, where I is the product intensity as a function of velocity (u) and CM angle (θ), provides a comprehensive description of the scattering dynamics.

Geometric structures of reactants, products, intermediates, and transition states on the triplet PES accessed by the C(^{3}P) + C_5H_6 reaction were optimized using the long-range corrected hybrid ωB97X-D density functional[56] with Pople's split-valence 6-311G(d,p) basis set;[57] vibrational frequencies were evaluated at the same level of theory following geometry optimizations. These calculations employed the GAUSSIAN 16 software package.[58] The ωB97X-D/6-311G(d,p) level of theory typically predicts bond lengths and bond angles with an

https://doi.org/10.1021/acs.jpclett.6c03038
J. Phys. Chem. Lett. 2026, 17, 12367−12375

accuracy of 0.01−0.02 Å and 1.0°, respectively, but is not sufficiently accurate for evaluation of relative energies. To achieve chemically accurate energetics, single-point energies of all optimized stationary points on the PES were refined using the explicitly correlated coupled-cluster method with single and double excitations and a perturbative treatment of triple excitations, CCSD(T)-F12/cc-pVQZ-F12,[59,60] with a correlation-consistent polarized valence quadruple-ζ basis set[61] optimized for use with F12 methods, using the MOLPRO 2021 program package.[62] The final level of theory was thus CCSD(T)-F12/cc-pVQZ-F12//ωB97X-D/6-311G(d,p) including zero-point vibrational energy corrections (ZPE) obtained at ωB97X-D/6-311G(d,p). At this level, the mean absolute error (MAE) for reaction energies is typically within 2−4 kJ mol^{-1}.[63]

Energy-dependent rate constants for unimolecular reaction steps following formation of initial intermediates in entrance reaction channels were computed using Rice−Ramsperger−Kassel−Marcus (RRKM) theory[64] utilizing molecular parameters and energies derived from the PES. The rate constants for each elementary step were evaluated in the zero-pressure limit, consistent with the conditions of low-density astrochemical environments. The rate constants were subsequently used to determine product branching ratios through the solution of the coupled reaction kinetic equations.[65] Our in-house UNIMOL code was employed in the calculations of RRKM rate constants and product branching ratios.[66]

■ ASSOCIATED CONTENT

Supporting Information

The Supporting Information is available free of charge at https://pubs.acs.org/doi/10.1021/acs.jpclett.6c03038.

Time of flight (TOF) mass spectra for the C+c-C_5H_6 reaction at m/z = 76 and 77, formation and role of intermediates **i3** and **i8**, complete PES including **i3** and **i8**, experimental parameters, RRKM rate constants, contributions to for the formation of phenyl radicals from **i4**−**i7**, and Cartesian coordinates and frequencies of all species (PDF)

■ AUTHOR INFORMATION

Corresponding Authors

Ralf I. Kaiser − *Department of Chemistry, University of Hawai'i at Manoa, Honolulu, Hawaii 96822, United States;* orcid.org/0000-0002-7233-7206; Email: ralfk@hawaii.edu

Alexander M. Mebel − *Department of Chemistry and Biochemistry, Florida International University, Miami, Florida 33199, United States;* orcid.org/0000-0002-7233-3133; Email: mebela@fiu.edu

Authors

Daniel González − *Department of Chemistry, University of Hawai'i at Manoa, Honolulu, Hawaii 96822, United States*

Ashleigh G. Hartwig − *Department of Chemistry and Biochemistry, Florida International University, Miami, Florida 33199, United States*

Surajit Metya − *Department of Chemistry, University of Hawai'i at Manoa, Honolulu, Hawaii 96822, United States;* orcid.org/0009-0004-5583-8481

Iakov A. Medvedkov − *Department of Chemistry, University of Hawai'i at Manoa, Honolulu, Hawaii 96822, United States;* orcid.org/0000-0003-0672-2090

Shane J. Goettl − *Department of Chemistry, University of Hawai'i at Manoa, Honolulu, Hawaii 96822, United States;* orcid.org/0000-0003-1796-5725

Complete contact information is available at: https://pubs.acs.org/10.1021/acs.jpclett.6c03038

Notes

The authors declare no competing financial interest.

■ ACKNOWLEDGMENTS

The experimental studies at the University of Hawai'i at Manoa were supported by the US Department of Energy, Basic Energy Sciences (DE-FG02-03ER15411).

■ REFERENCES

(1) McCarthy, M. C.; McGuire, B. A. Spectroscopic studies of polycyclic aromatic hydrocarbons: Interstellar aromatic chemistry revealed. *Annu. Rev. Phys. Chem.* **2026**, *77*, 345.

(2) Kaiser, R. I.; Parker, D. S.; Mebel, A. M. Reaction dynamics in astrochemistry: Low-temperature pathways to polycyclic aromatic hydrocarbons in the interstellar medium. *Annu. Rev. Phys. Chem.* **2015**, *66* (1), 43−67.

(3) Wenzel, G.; Gong, S.; Xue, C.; Changala, P. B.; Holdren, M. S.; Speak, T. H.; Stewart, D. A.; Fried, Z. T. P.; Willis, R. H. J.; Bergin, E. A.; Burkhardt, A. M.; Byrne, A. N.; Charnley, S. B.; Lipnicky, A.; Loomis, R. A.; Shingledecker, C. N.; Cooke, I. R.; McCarthy, M. C.; Remijan, A. J.; Wendlandt, A. E.; McGuire, B. A. Discovery of the seven-ring polycyclic aromatic hydrocarbon cyanocoronene ($C_{24}H_{11}CN$) in GOTHAM observations of TMC-1. *Astrophys. J. Lett.* **2025**, *984* (1), L36.

(4) Schmitt-Kopplin, P.; Gabelica, Z.; Gougeon, R. D.; Fekete, A.; Kanawati, B.; Harir, M.; Gebefuegi, I.; Eckel, G.; Hertkorn, N. High molecular diversity of extraterrestrial organic matter in Murchison meteorite revealed 40 years after its fall. *Proc. Natl. Acad. Sci. U. S. A.* **2010**, *107* (7), 2763−2768.

(5) Glavin, D. P.; Dworkin, J. P.; O'D Alexander, C. M.; Aponte, J. C.; Baczynski, A. A.; Barnes, J. J.; Bechtel, H. A.; Berger, E. L.; Burton, A. S.; Caselli, P.; Chung, A. H.; Clemett, S. J.; Cody, G. D.; Dominguez, G.; Elsila, J. E.; Farnsworth, K. K.; Foustoukos, D. I.; Freeman, K. H.; Furukawa, Y.; Gainsforth, Z.; Graham, H. V.; Grassi, T.; Giuliano, B. M.; Hamilton, V. E.; Haenecour, P.; Heck, P. R.; Hofmann, A. E.; House, C. H.; Huang, Y.; Kaplan, H. H.; Keller, L. P.; Kim, B.; Koga, T.; Liss, M.; McLain, H. L.; Marcus, M. A.; Matney, M.; McCoy, T. J.; McIntosh, O. M.; Mojarro, A.; Naraoka, H.; Nguyen, A. N.; Nuevo, M.; Nuth, J. A.; Oba, Y.; Parker, E. T.; Peretyazhko, T. S.; Sandford, S. A.; Santos, E.; Schmitt-Kopplin, P.; Seguin, F.; Simkus, D. N.; Shahid, A.; Takano, Y.; Thomas-Keprta, K. L.; Tripathi, H.; Weiss, G.; Zheng, Y.; Lunning, N. G.; Righter, K.; Connolly, H. C.; Lauretta, D. S. Abundant ammonia and nitrogen-rich soluble organic matter in samples from asteroid (101955) Bennu. *Nat. Astron.* **2025**, *9* (2), 199−210.

(6) Lauretta, D. S.; Connolly, H. C.; Aebersold, J. E.; O'D Alexander, C. M.; Ballouz, R.-L.; Barnes, J. J.; Bates, H. C.; Bennett, C. A.; Blanche, L.; Blumenfeld, E. H.; Clemett, S. J.; Cody, G. D.; DellaGiustina, D. N.; Dworkin, J. P.; Eckley, S. A.; Foustoukos, D. I.; Franchi, I. A.; Glavin, D. P.; Greenwood, R. C.; Haenecour, P.; Hamilton, V. E.; Hill, D. H.; Hiroi, T.; Ishimaru, K.; Jourdan, F.; Kaplan, H. H.; Keller, L. P.; King, A. J.; Koefoed, P.; Kontogiannis, M. K.; Le, L.; Macke, R. J.; McCoy, T. J.; Milliken, R. E.; Najorka, J.; Nguyen, A. N.; Pajola, M.; Polit, A. T.; Righter, K.; Roper, H. L.; Russell, S. S.; Ryan, A. J.; Sandford, S. A.; Schofield, P. F.; Schultz, C. D.; Seifert, L. B.; Tachibana, S.; Thomas-Keprta, K. L.; Thompson, M. S.; Tu, V.; Tusberti, F.; Wang, K.; Zega, T. J.; Wolner, C. W. V.

Asteroid (101955) Bennu in the laboratory: Properties of the sample collected by OSIRIS-REx. *Meteorit. Planet. Sci.* **2024**, *59* (9), 2453−2486.
(7) Tielens, A. G. Interstellar polycyclic aromatic hydrocarbon molecules. *Annu. Rev. Astron. Astrophys.* **2008**, *46* (1), 289−337.
(8) Tielens, A.; Van Kerckhoven, C.; Peeters, E.; Hony, S. In Interstellar and Circumstellar PAHs. In *Symposium-International Astronomical Union*; , Cambridge University Press, 2000; pp 349−362.
(9) Cherchneff, I.; Barker, J. R.; Tielens, A. G. Polycyclic aromatic hydrocarbon formation in carbon-rich stellar envelopes. *Astrophys. J.* **1992**, *401*, 269−287.
(10) Cohen, M.; Tielens, A.; Bregman, J. Mid-infrared spectra of WC 9 stars-The composition of circumstellar and interstellar dust. *Astrophys. J.* **1989**, *344*, L13−L16.
(11) Micelotta, E.; Jones, A.; Tielens, A. Polycyclic aromatic hydrocarbon processing in interstellar shocks. *Astron. Astrophys.* **2010**, *510*, A36.
(12) Tielens, A. The molecular universe. *Rev. Mod. Phys.* **2013**, *85* (3), 1021−1081.
(13) Frenklach, M.; Feigelson, E. D. Formation of polycyclic aromatic hydrocarbons in circumstellar envelopes. *Astrophys. J.* **1989**, *341*, 372−384.
(14) Zenobi, R.; Philippoz, J.-M.; Zare, R. N.; Buseck, P. R. Spatially resolved organic analysis of the Allende meteorite. *Science* **1989**, *246* (4933), 1026−1029.
(15) Kaiser, R. I.; Hansen, N. An aromatic universe-A physical chemistry perspective. *J. Phys. Chem. A* **2021**, *125* (18), 3826−3840.
(16) Zhao, L.; Prendergast, M. B.; Kaiser, R. I.; Xu, B.; Ablikim, U.; Ahmed, M.; Sun, B.-J.; Chen, Y.-L.; Chang, A. H. H.; Mohamed, R. K.; Fischer, F. R. Synthesis of polycyclic aromatic hydrocarbons by phenyl addition-dehydrocyclization: The third way. *Angew. Chem.* **2019**, *131* (48), 17603−17611.
(17) Parker, D. S.; Zhang, F.; Kim, Y. S.; Kaiser, R. I.; Landera, A.; Kislov, V. V.; Mebel, A. M.; Tielens, A. Low temperature formation of naphthalene and its role in the synthesis of PAHs (polycyclic aromatic hydrocarbons) in the interstellar medium. *Proc. Natl. Acad. Sci. U. S. A.* **2012**, *109* (1), 53−58.
(18) Parker, D. D. S.; Zhang, D. F.; Kaiser, D. R. I.; Kislov, D. V. V.; Mebel, D. A. M. Indene Formation under Single-Collision Conditions from the Reaction of Phenyl Radicals with Allene and Methylacetylene—A Crossed Molecular Beam and Ab Initio Study. *Chem.—Asian J.* **2011**, *6* (11), 3035−3047.
(19) Mebel, A. M.; Landera, A.; Kaiser, R. I. Formation mechanisms of naphthalene and indene: From the interstellar medium to combustion flames. *J. Phys. Chem. A* **2017**, *121* (5), 901−926.
(20) Zhao, L.; Kaiser, R. I.; Xu, B.; Ablikim, U.; Ahmed, M.; Evseev, M. M.; Bashkirov, E. K.; Azyazov, V. N.; Mebel, A. M. Low-temperature formation of polycyclic aromatic hydrocarbons in Titan's atmosphere. *Nat. Astron.* **2018**, *2* (12), 973−979.
(21) Zhao, L.; Kaiser, R. I.; Xu, B.; Ablikim, U.; Ahmed, M.; Evseev, M. M.; Bashkirov, E. K.; Azyazov, V. N.; Mebel, A. M. A unified mechanism on the formation of acenes, helicenes, and phenacenes in the gas phase. *Angew. Chem.* **2020**, *132* (10), 4080−4087.
(22) Parker, D. S.; Kaiser, R. I.; Bandyopadhyay, B.; Kostko, O.; Troy, T. P.; Ahmed, M. Unexpected chemistry from the reaction of naphthyl and acetylene at combustion-like temperatures. *Angew. Chem., Int. Ed.* **2015**, *54* (18), 5421−5424.
(23) Hamadi, A.; Sun, W.; Abid, S.; Chaumeix, N.; Comandini, A. An experimental and kinetic modeling study of benzene pyrolysis with C2- C3 unsaturated hydrocarbons. *Combust. Flame* **2022**, *237*, 111858.
(24) Mitra, T.; Zhang, T.; Sediako, A. D.; Thomson, M. J. Understanding the formation and growth of polycyclic aromatic hydrocarbons (PAHs) and young soot from n-dodecane in a sooting laminar coflow diffusion flame. *Combust. Flame* **2019**, *202*, 33−42.
(25) Zhang, F.; Jones, B.; Maksyutenko, P.; Kaiser, R. I.; Chin, C.; Kislov, V. V.; Mebel, A. M. Formation of the phenyl radical [C_6H_5 (X^2A_1)] under single collision conditions: A crossed molecular beam and ab initio study. *J. Am. Chem, Soc.* **2010**, *132* (8), 2672−2683.
(26) Zhao, L.; Lu, W.; Ahmed, M.; Zagidullin, M. V.; Azyazov, V. N.; Morozov, A. N.; Mebel, A. M.; Kaiser, R. I. Gas-phase synthesis of benzene via the propargyl radical self-reaction. *Sci. Adv.* **2021**, *7* (21), No. eabf0360.
(27) Kaiser, R. I. Experimental investigation on the formation of carbon-bearing molecules in the interstellar medium via neutral-neutral reactions. *Chem. Rev.* **2002**, *102* (5), 1309−1358.
(28) Kaiser, R. I.; Mebel, A. M. The reactivity of ground-state carbon atoms with unsaturated hydrocarbons in combustion flames and in the interstellar medium. *Int. Rev. Phys. Chem.* **2002**, *21* (2), 307−356.
(29) Kaiser, R. I.; Ochsenfeld, C.; Stranges, D.; Head-Gordon, M.; Lee, Y. Combined crossed molecular beams and ab initio investigation of the formation of carbon-bearing molecules in the interstellar medium via neutral-neutral reactions. *Faraday Discuss.* **1998**, *109*, 183−204.
(30) Haider, N.; Husain, D. The Collisional Behaviour of Ground State Atomic Carbon, C ($2p^2$ (^3P_J)), with Unsaturated Cyclic Compounds Studied by Time-Resolved Atomic Resonance Absorption Spectroscopy in the Vacuum Ultra-Violet. *Ber. Bunsen-Ges. Phys. Chem.* **1993**, *97* (4), 571−576.
(31) Miller, W.; Safron, S.; Herschbach, D. Exchange reactions of alkali atoms with alkali halides: A collision complex mechanism. *Discuss. Faraday Soc.* **1967**, *44*, 108−122.
(32) Levine, R. D.; Bernstein, R. B. *Molecular Reaction Dynamics and Chemical Reactivity*; Oxford University Press: Oxford, 1987.
(33) Gu, X.; Guo, Y.; Zhang, F.; Mebel, A. M.; Kaiser, R. I. Reaction dynamics of carbon-bearing radicals in circumstellar envelopes of carbon stars. *Faraday Discuss.* **2006**, *133*, 245−275.
(34) Ruscic, B.; Bross, D. H., *Active Thermochemical Tables (ATcT) Values Based on ver. 1.220 of the Thermochemical Network*; Argonne National Laboratory, 2025.
(35) Kaiser, R.; Stranges, D.; Lee, Y.; Suits, A. Neutral-neutral reactions in the interstellar medium. I. Formation of carbon hydride radicals via reaction of carbon atoms with unsaturated hydrocarbons. *Astrophys. J.* **1997**, *477* (2), 982−989.
(36) Kaiser, R.; Sun, W.; Suits, A.; Lee, Y. Crossed beam reaction of atomic carbon, C (^3P_j), with the propargyl radical, C_3H_3 (X^2B_2): Observation of diacetylene, C_4H_2 ($X^1\Sigma_g^+$). *J. Chem. Phys.* **1997**, *107* (20), 8713−8716.
(37) Zhang, F.; Kim, Y. S.; Zhou, L.; Chang, A. H.; Kaiser, R. I. A crossed molecular beam study on the synthesis of the interstellar 2, 4-pentadiynylidyne radical (HCCCCC). *J. Chem. Phys.* **2008**, *129* (13), 134313.
(38) Parker, D. S.; Zhang, F.; Kim, Y. S.; Kaiser, R. I.; Mebel, A. M. On the Formation of Resonantly Stabilized C_5H_3 Radicals— A Crossed Beam and Ab Initio Study of the Reaction of Ground State Carbon Atoms with Vinylacetylene. *J. Phys. Chem. A* **2011**, *115* (5), 593−601.
(39) Hahndorf, I.; Lee, H.; Mebel, A.; Lin, S.; Lee, Y.; Kaiser, R. A combined crossed beam and ab initio investigation on the reaction of carbon species with C_4H_6 isomers. I. The 1,3-butadiene molecule, $H_2CCHCHCH_2$ (X^1A'). *J. Chem. Phys.* **2000**, *113* (21), 9622−9636.
(40) Huang, L.; Lee, H.; Mebel, A.; Lin, S.; Lee, Y.; Kaiser, R. A combined crossed beam and ab initio investigation on the reaction of carbon species with C_4H_6 isomers. II. The dimethylacetylene molecule, H_3CCCCH_3 (X^1A_{1g}). *J. Chem. Phys.* **2000**, *113* (21), 9637−9648.
(41) Hahndorf, I.; Lee, Y.; Kaiser, R.; Vereecken, L.; Peeters, J.; Bettinger, H.; Schreiner, P.; Schleyer, P. v. R.; Allen, W.; Schaefer, H., III A combined crossed-beam, ab initio, and Rice-Ramsperger-Kassel-Marcus investigation of the reaction of carbon atoms C (^3P_j) with benzene, C_6H_6 (X^1A_{1g}) and d_6-benzene, C_6D_6 (X^1A_{1g}). *J. Chem. Phys.* **2002**, *116* (8), 3248−3262.
(42) Yang, Z.; Galimova, G. R.; He, C.; Goettl, S. J.; Paul, D.; Lu, W.; Ahmed, M.; Mebel, A. M.; Li, X.; Kaiser, R. I. Gas-phase formation of the resonantly stabilized 1-indenyl ($C_9H_7\bullet$) radical in the interstellar medium. *Sci. Adv.* **2023**, *9* (36), No. eadi5060.
(43) Yang, Z.; Galimova, G. R.; He, C.; Goettl, S. J.; Li, X.; Mebel, A. M.; Kaiser, R. I. An Unconventional Dark Radical Chemistry in Dense

https://doi.org/10.1021/acs.jpclett.6c03038
J. Phys. Chem. Lett. 2026, 17, 12367−12375

Molecular Clouds: Directed Gas-Phase Formation of Naphthyl Radicals. *J. Am. Chem, Soc.* **2025**, *147* (51), 47359−47369.
(44) Mebel, A.; Kislov, V.; Hayashi, M. Prediction of product branching ratios in the $C(^3P) + C_2H_2 \rightarrow l\text{-}C_3H + H/c\text{-}C_3H + H/C_3 + H_2$ reaction using ab initio coupled clusters calculations extrapolated to the complete basis set combined with Rice-Ramsperger-Kassel-Marcus and radiationless transition theories. *J. Chem. Phys.* **2007**, *126* (20), 204310.
(45) Frenklach, M.; Jasper, A. W.; Mebel, A. M. Phenalenyl growth reactions and implications for prenucleation chemistry of aromatics in flames. *Phys. Chem. Chem. Phys.* **2024**, *26* (17), 13034−13048.
(46) Madden, L.; Moskaleva, L.; Kristyan, S.; Lin, M.-C. Ab initio MO study of the unimolecular decomposition of the phenyl radical. *J. Phys. Chem. A* **1997**, *101* (36), 6790−6797.
(47) Chastaing, D.; James, P. L.; Sims, I. R.; Smith, I. W. M. Neutral-neutral reactions at the temperatures of interstellar clouds: Rate coefficients for reactions of atomic carbon, C (^3P), with O_2, C_2H_2, C_2H_4 and C_3H_6 down to 15 K. *Phys. Chem. Chem. Phys.* **1999**, *1* (9), 2247−2256.
(48) Haider, N.; Husain, D. Absolute rate data for the reactions of ground-state atomic carbon, C [$2p^2$ (^3P_J)], with alkenes investigated by time-resolved atomic resonance absorption spectroscopy in the vacuum ultraviolet. *J. Chem. Soc., Faraday Trans.* **1993**, *89* (1), 7−14.
(49) Zhao, L.; Kaiser, R. I.; Xu, B.; Ablikim, U.; Ahmed, M.; Zagidullin, M. V.; Azyazov, V. N.; Howlader, A. H.; Wnuk, S. F.; Mebel, A. M. VUV photoionization study of the formation of the simplest polycyclic aromatic hydrocarbon: Naphthalene ($C_{10}H_8$). *J. Phys. Chem. Lett.* **2018**, *9* (10), 2620−2626.
(50) Zhao, L.; Kaiser, R. I.; Xu, B.; Ablikim, U.; Lu, W.; Ahmed, M.; Evseev, M. M.; Bashkirov, E. K.; Azyazov, V. N.; Zagidullin, M. V.; Morozov, A. N.; Howlader, A. H.; Wnuk, S. F.; Mebel, A. M.; Joshi, D.; Veber, G.; Fischer, F. R. Gas phase synthesis of [4]-helicene. *Nat. Commun.* **2019**, *10* (1), 1510.
(51) Gu, X.; Guo, Y.; Kaiser, R. I. Mass spectrum of the butadiynyl radical (C_4H; $X^2\sum^+$). *Int. J. Mass spectrom.* **2005**, *246* (1−3), 29−34.
(52) Moffett, R. B. Cyclopentadiene and 3-Chlorocyclopentene. *Organic Syntheses* **1952**, *32*, 41−44.
(53) Yang, Z.; Fujioka, K.; Galimova, G. R.; Medvedkov, I. A.; Goettl, S. J.; Sun, R.; Mebel, A. M.; Kaiser, R. I. Directed Gas-Phase Formation of Azulene ($C_{10}H_8$): Unraveling the Bottom-Up Chemistry of Saddle-Shaped Aromatics. *ACS Cent. Sci.* **2025**, *11* (2), 322−330.
(54) Vernon, M. F. *Molecular Beam Scattering*; University of California: Berkeley, CA, 1983.
(55) Weiss, P. S. *Reaction Dynamics of Electronically Excited Alkali Atoms with Simple Molecules*; University of California, Berkeley, CA, 1986.
(56) Chai, J.-D.; Head-Gordon, M. Long-range corrected hybrid density functionals with damped atom-atom dispersion corrections. *Phys. Chem. Chem. Phys.* **2008**, *10* (44), 6615−6620.
(57) Krishnan, R.; Binkley, J. S.; Seeger, R.; Pople, J. A. Self-consistent molecular orbital methods. XX. A basis set for correlated wave functions. *J. Chem. Phys.* **1980**, *72* (1), 650−654.
(58) Frisch, G.; Schlegel, H.; Scuseria, G.; Robb, M.; Cheeseman, J.; Scalmani, G.; Barone, V.; Petersson, G.; Nakatsuji, H.; Li, X., et al. Gaussian 16, Revision C. 01; Gaussian, Inc.: Wallington, CT, 2016.
(59) Adler, T. B.; Knizia, G.; Werner, H.-J. A simple and efficient CCSD (T)-F12 approximation. *J. Chem. Phys.* **2007**, *127* (22), 221106.
(60) Knizia, G.; Adler, T. B.; Werner, H.-J. Simplified CCSD (T)-F12 methods: Theory and benchmarks. *J. Chem. Phys.* **2009**, *130* (5), 054104.
(61) Dunning, T. H., Jr Gaussian basis sets for use in correlated molecular calculations. I. The atoms boron through neon and hydrogen. *J. Chem. Phys.* **1989**, *90* (2), 1007−1023.
(62) Werner, H.; Knowles, P.; Celani, P.; Györffy, W.; Hesselman, A.; Kats, D.; Knizia, G.; Köhn, A.; Korona, T.; Kreplin, D.; Lindh, R.; Ma, Q.; Manby, F.; Mitrushenkov, A.; Rauhut, G.; Schütz, M.; Shamasundar, K.; Adler, T.; Amos, R.; Bennie, S.; Bernhardsson, A.; Berning, A.; Black, J.; Bygrave, P.; Cimiraglia, R.; Cooper, D.; Coughtrie, D.; Deegan, M.; Dobbyn, A.; Doll, K.; Dornbach, M.; Eckert, F.; Erfort, S.; Goll, E.; Hampel, C.; Hetzer, G.; Hill, J.; Hodges, M.; Hrenar, T.; Jansen, G.; Köppl, C.; Kollmar, C.; Lee, S.; Liu, Y.; Lloyd, A.; Mata, R.; May, A.; Mussard, B.; McNicholas, S.; Meyer, W.; Iii, T.; Mura, M.; Nicklass, A.; O'Neill, D.; Palmieri, P.; Peng, D.; Peterson, K. A.; Pflüger, K.; Pitzer, R.; Polyak, I.; Reiher, M.; Richardson, J.; Robinson, J.; Schröder, B.; Schwilk, M.; Shiozaki, T.; Sibaev, M.; Stoll, H.; Stone, A.; Tarroni, R.; Thorsteinsson, T.; Toulouse, J.; Wang, M.; Welborn, M.; Ziegler, B. *MOLPRO, a Package of Ab Initio Programs*, version 2021.2, 2021.
(63) Zhang, J.; Valeev, E. F. Prediction of reaction barriers and thermochemical properties with explicitly correlated coupled-cluster methods: A basis set assessment. *J. Chem. Theory Comput.* **2012**, *8* (9), 3175−3186.
(64) Steinfeld, J. I.; Francisco, J. S.; Hase, W. L. *Chemical Kinetics and Dynamics*; Prentice Hall: Upper Saddle River, NJ, 1999; Vol. 2.
(65) Kislov, V.; Nguyen, T.; Mebel, A.; Lin, S.; Smith, S. Photodissociation of benzene under collision-free conditions: An ab initio/Rice-Ramsperger-Kassel-Marcus study. *J. Chem. Phys.* **2004**, *120* (15), 7008−7017.
(66) He, C.; Zhao, L.; Thomas, A. M.; Morozov, A. N.; Mebel, A. M.; Kaiser, R. I. Elucidating the chemical dynamics of the elementary reactions of the 1-propynyl radical (CH_3CC; X^2A_1) with methylacetylene (H_3CCCH; X^1A_1) and allene (H_2CCCH_2; X^1A_1). *J. Phys. Chem. A* **2019**, *123* (26), 5446−5462.

https://doi.org/10.1021/acs.jpclett.6c03038
J. Phys. Chem. Lett. 2026, 17, 12367−12375